

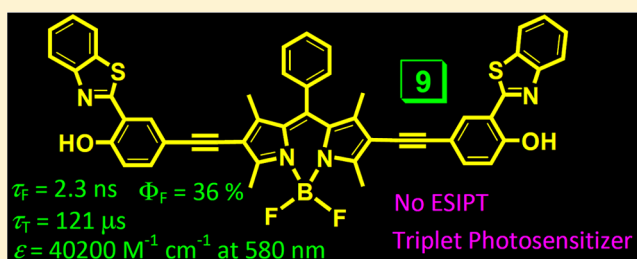
Accessing the Long-Lived Triplet Excited States in Bodipy-Conjugated 2-(2-Hydroxyphenyl) Benzothiazole/Benzoxazoles and Applications as Organic Triplet Photosensitizers for Photooxidations

Pei Yang, Jianzhang Zhao,* Wanhua Wu, Xuerong Yu, and Yifan Liu

State Key Laboratory of Fine Chemicals, School of Chemical Engineering, Dalian University of Technology, E-208 West Campus, 2 Ling-Gong Road, Dalian 116024, P. R. China

S Supporting Information

ABSTRACT: Bodipy derivatives containing excited state intramolecular proton transfer (ESIPT) chromophores 2-(2-hydroxyphenyl) benzothiazole and benzoxazole (HBT and HBO) subunits were prepared (7–10). The compounds show red-shifted UV–vis absorption (530–580 nm; ϵ up to 50000 $\text{M}^{-1} \text{cm}^{-1}$) and emission compared to both HBT/HBO and Bodipy. The new chromophores show *small* Stokes shift (45 nm) and *high* fluorescence quantum yields (Φ_F up to 36%), which are in stark contrast to HBT and HBO (Stokes shift up to 180 nm and Φ_F as low as 0.6%). On the basis of steady state and time-resolved absorption spectroscopy, as well as DFT/TDDFT calculations, we propose that 7–9 do not undergo ESIPT upon photoexcitation. Interestingly, nanosecond time-resolved transient absorption spectroscopy demonstrated that Bodipy-localized triplet excited states were populated for 7–10 upon photoexcitation; the lifetimes of the triplet excited states (τ_T) are up to 195 μs . DFT calculations confirm the transient absorptions are due to the triplet state. Different from the previous report, we demonstrated that population of the triplet excited states is not the result of ESIPT. The compounds were used as organic triplet photosensitizers for photooxidation of 1,5-dihydroxynaphthalene. One of the compounds is more efficient than the conventional $[\text{Ir}(\text{ppy})_2(\text{phen})][\text{PF}_6]$ triplet photosensitizer. Our result will be useful for design of new Bodipy derivatives, ESIPT compounds, and organic triplet photosensitizers, as well as for applications of these compounds in photovoltaics, photocatalysis and luminescent materials, etc.



1. INTRODUCTION

Excited state intramolecular proton transfer (ESIPT) has attracted much attention^{1–4} due to applications in fluorescent molecular probes,^{3,4} molecular logic gates,^{1,4,5} fluorescent bioimaging,⁶ and light-emitting materials,^{2,3,7–9} as well as for photophysical studies.^{1,9–15} The typical ESIPT chromophores are those containing 2-(2-hydroxyphenyl) benzothiazole (HBT) or 2-(2-hydroxyphenyl) benzoxazole units (HBO) (Scheme 1).¹⁶ Furthermore, these ESIPT chromophores are usually limited to those with a small π -conjugation framework, and thus the absorption are in UV or blue range,^{2,7,9–11,13,16–19} which is detrimental to their applications in molecular probes or photoluminescent dyes.^{2–4,12} ESIPT chromophores with a larger π -conjugation framework are expected to show red-shifted absorption. However, very few such ESIPT chromophores have been reported.^{2,14,18,20}

We noticed that one interesting property of ESIPT chromophores has not yet been explored, that is, the population of *triplet* excited states upon photoexcitation.^{12,16,18}

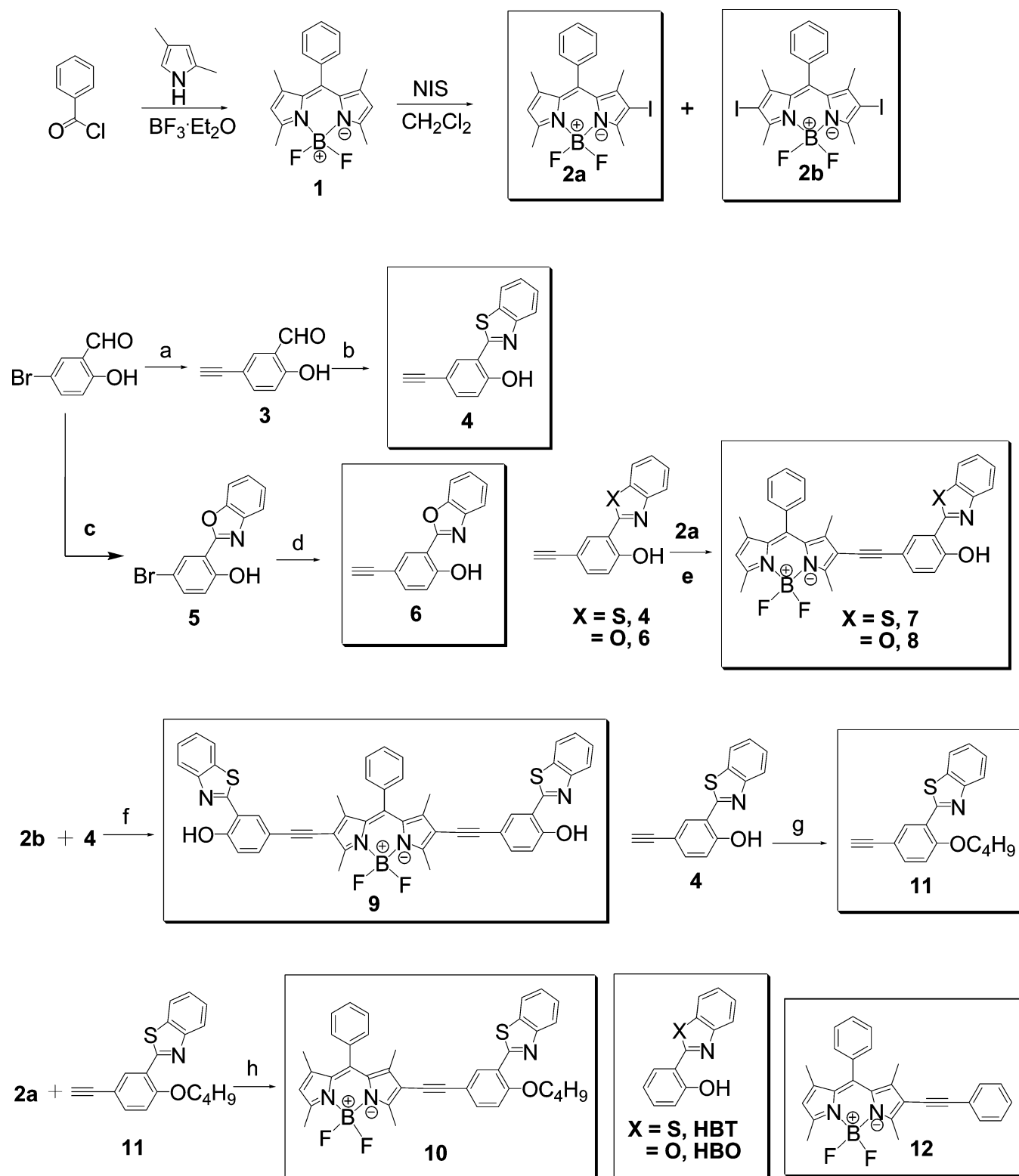
This is a remarkable feature because very often the triplet excited state of the heavy-atom-free organic chromophores cannot be efficiently populated upon photoexcitation. $S_0 \rightarrow T_1$ is a quantum mechanically forbidden transition, and the intersystem crossing (ISC) is usually difficult without heavy

atom effect.^{21–24} However, it should be pointed out that exceptions do exist, for example, benzophenone and biacetyl undergo efficient ISC upon photoexcitation. For most aromatic hydrocarbon, the major nonradiative decay channel of the S_1 state is the intersystem crossing, not internal conversion, and the same is also true for compounds like methylene blue. Although sporadic heavy-atom-free organic triplet photosensitizers do exist, such as porphyrins, etc.,^{22,25a,b} the photophysics of these compounds is elusive, and it is difficult to *design* an organic chromophore to show the *predetermined* ISC property. Organic chromophores with triplet excited states populated upon photoexcitation can be used for photovoltaics, photocatalysis,²⁶ and photodynamic therapy (PDT).^{25a,b,27}

On the other hand, boron-dipyrromethene (Bodipy) is a versatile fluorophore, due to its strong absorption of visible light (ϵ up to 80000 $\text{M}^{-1} \text{cm}^{-1}$ at 504 nm for the unsubstituted Bodipy), high fluorescence quantum yields (close to unity), and good photostability.^{28–31} Moreover, the rich chemistry of Bodipy allows feasible derivatization.^{25,28b,32} Bodipy was widely used for construction of molecular probes.^{25b,g,30} However, to

Received: May 10, 2012

Published: June 28, 2012

Scheme 1. Synthesis of Bodipy-Derived Chromophores 7–10^a

^aKey: (a) $\text{PdCl}_2(\text{PPh}_3)_2$, PPh_3 , CuI , NEt_3 , ethynyltrimethylsilane, argon atmosphere, 80°C , 3 h; then $(n\text{-Bu})_4\text{NF}/\text{THF}$, room temperature, 10 min; 54%. (b) 2-Aminothiophenol, CH_3OH , room temperature, 12 h; 30%. (c) 2-Aminophenol, acetic acid, $\text{Pb}(\text{OAc})_4$, room temperature 30 min, then 110°C , 1 h; 60%. (d) $\text{PdCl}_2(\text{PPh}_3)_2$, PPh_3 , CuI , NEt_3 , ethynyltrimethylsilane, argon atmosphere, 80°C , 4 h; then K_2CO_3 , CH_3OH , CH_2Cl_2 , room temperature, 6 h; 35%. (e) $\text{Pd}(\text{PPh}_3)_4$, CuI , NEt_3 , THF , argon atmosphere, 60°C , 6 h; yield: 40% for compound **7**, 10% for compound **8**. (f) $\text{Pd}(\text{PPh}_3)_4$, CuI , NEt_3 , THF , argon atmosphere, 60°C , 8 h; 25%. (g) $n\text{-C}_4\text{H}_9\text{Br}$, DMF , 50°C , 4 h; 86%. (h) $\text{PdCl}_2(\text{PPh}_3)_2$, PPh_3 , CuI , NEt_3 , argon atmosphere, 60°C , 6 h; 36%.

the best of our knowledge, ESIPT chromophores containing Bodipy units have never been reported.^{1–3}

To address the above challenges, we selected Bodipy to extend the π -conjugation of the conventional ESIPT chromophores such as HBT and HBO.

Herein we devised Bodipy-conjugated 2-(2-hydroxyphenyl) benzothiazole (HBT) or 2-(2-hydroxyphenyl) benzoxazole units (HBO) chromophores (7–10, Scheme 1). These dyes show strong absorption of visible light (ϵ up to 50000 M⁻¹ cm⁻¹ at 530–580 nm) and intense fluorescence (Φ_F up to 36%). Long-lived triplet excited states were observed for 7–10. Triplet excited states of bromine- or iodine-containing Bodipy derivatives have been reported.^{21,23,24} However, population of the triplet excited state was rarely reported for heavy-atom-free Bodipy.^{25a,b} On the basis of steady state and time-resolved spectroscopy, as well as DFT calculations, we propose that no ESIPT occurs for compounds 7–10.

Importantly, we found that the population of triplet excited state is not the result of ESIPT.¹⁸ The compounds were used as singlet oxygen (¹O₂) sensitizers for the photooxidation of 1,5-dihydroxynaphthalene (DHN).²⁶ These organic triplet photosensitizers are proved more efficient than the conventional transition metal complex triplet sensitizer, such as [Ir(ppy)₂(phen)][PF₆].²⁶ Organic chromophores with room temperature long-lived triplet excited states populated upon photoexcitation are rare, and our studies are useful for designing new organic triplet sensitizers for applications in photovoltaics, photocatalysis,²⁶ singlet oxygen (¹O₂) photosensitizing,^{21,23,25a,b} and upconversion,^{33,34} etc.

2. RESULTS AND DISCUSSION

2.1. Design and Synthesis of the Compounds.

Our strategy of molecular design lies in two notions. First, with extension of the π -conjugation framework of HBT and HBO, the UV–vis absorption will be red-shifted. Second, we postulate that population of the T₁ excited state upon excitation may be retained in the new compounds.

Our approach is to connect the HBT or HBO units with the Bodipy moiety via C \equiv C triplet bonds. 4,4-Difluoro-1,3,5,7-tetramethyl-8-phenyl-4-bora-3a,4a-diaza-s-indacene (Bodipy) was used as the starting material (Scheme 1). Mono- and bis-iodination of the Bodipy by *N*-iodo-succinimide (NIS) gave compounds **2a** and **2b**. The ethynylated HBO or the HBT units were obtained by 5-bromosacaldehyde through Sonogashira cross-coupling reactions. Target compounds 7–9 were obtained by Pd(0)-catalyzed Sonogashira coupling of the respective components (Scheme 1). The effect of the one-atom substituent (O/S) was investigated with compounds 7 and 8. Compound **10** was prepared as a control compound. The hydroxyl group in **10** was alkylated, to exclude any ESIPT effect. All the compounds were obtained in moderate to satisfying yields.

2.2. Steady-State UV–vis Absorption and Emission Spectra. The UV–vis absorption of the compounds was studied (Figure 1a). The ethynylated HBO and HBT show absorption at 335 and 349 nm, respectively. For the Bodipy-conjugated chromophores, however, the absorption maximum are remarkably red-shifted.^{14,18} For example, the absorption of **7** is at 535 nm ($\epsilon = 57000$ M⁻¹ cm⁻¹). Compound **8** gives the same absorption feature, implying that the effect of the singlet atom substitution of S vs O is small under this circumstance (Figure 1b). With a larger π -conjugation framework, **9** shows red-shifted absorption at 580 nm ($\epsilon = 40000$ M⁻¹ cm⁻¹). The

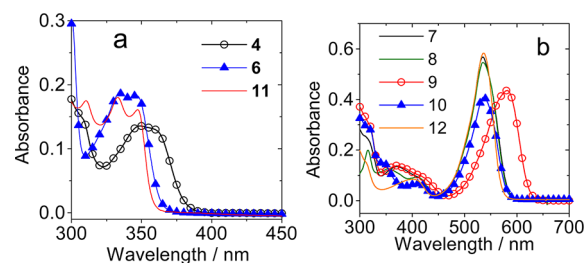


Figure 1. UV–vis absorption of the compounds (in toluene); $c = 1.0 \times 10^{-5}$ M, 20 °C.

new compounds show red-shifted absorption compared to the unsubstituted Bodipy, and thus the π -conjugation between the Bodipy core and the HBT and HBO moieties are efficient. It should be pointed out that the Bodipy and the benzothiazole moieties are at the *meso* position to each other, which may diminish the π -conjugation to some extent. The absorption of the compounds is similar to that of 2-phenylethynyl-substituted Bodipy (compound **12**), indicating the effect of HBT or HBO units on the absorption is not significant. With alkylation of the hydroxyl group, **11** shows slightly blue-shifted absorption compared to **4**. Interestingly, the alkylation of the hydroxyl moiety does not change the UV–vis absorption dramatically for the compounds with large π -conjugation framework; for example, **10** shows absorption similar to that of **7** (Figure 1b).

The compounds 7–10 show emission in the range of 580–620 nm (Figure 2), which are red-shifted vs HBO and HBT

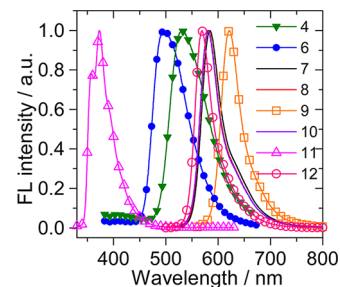


Figure 2. Fluorescence emission spectra of compounds **4** and **6–12** (in toluene); $c = 1.0 \times 10^{-5}$ M, 20 °C.

(530 nm)¹⁶ and the unsubstituted Bodipys ($\lambda_{em} = 510$ –530 nm). Compounds **7**, **8**, and **9** show *small* Stokes shifts (ca. 45 nm). On the contrary, **4** and **6** show large Stokes shifts (160–180 nm), which are typical for ESIPT.² Thus we propose that ESIPT occurs for **4** and **6**, but not for **7–9**. This postulation was supported by the blue-shifted emission of **11**, for which the hydroxyl group was alkylated, and thus ESIPT is fully excluded. Compound **11** shows blue-shifted emission (374 nm) compared to **4** (531 nm). This blue-shifted emission (and small Stokes shift) is in agreement with the lack of ESIPT for **11**. For **4**, ESIPT occur upon photoexcitation (see later section). In stark contrast, **10** show similar emission wavelength compared to **7**. Thus we propose that **7** does *not* undergo ESIPT upon photoexcitation.

Compounds **4** and **6** show large Stokes shifts (180 and 160 nm, respectively),³⁵ and low fluorescence quantum yields of 0.002 and 0.027 (Table 2). These values are close to those of the unsubstituted HBT and HBO (0.006 and 0.02, respectively).³⁵ For the new Bodipy-based chromophores, however, the fluorescence quantum yields are much higher

(0.225, 0.202, and 0.360 for 7–9, respectively). The emissions of 7–10 were also recorded with excitation at shorter wavelength (330–360 nm, Figure S25), emission similar to that with longer excitation wavelength were observed, indicating that the emission of HBT or the HBO units were completely quenched in compounds 7–10. The quenching may be caused by intramolecular energy transfer to the Bodipy moiety.

2.3. Solvent-Dependency of the Emission. In nonprotic organic solvents, compound 4 shows emission at 530 nm. In protic solvent such as methanol, emission band at 420 nm was observed (Figure 3). In toluene, dichloromethane and ethyl

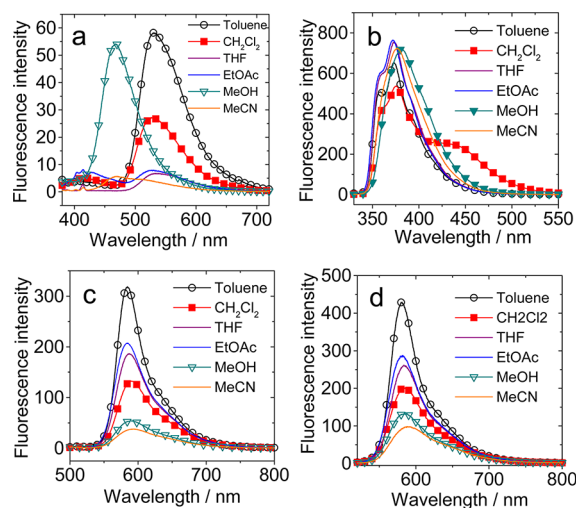


Figure 3. Fluorescence emission spectra of (a) 4 ($\lambda_{\text{ex}} = 370$ nm), (b) 11 ($\lambda_{\text{ex}} = 320$ nm), (c) 7 ($\lambda_{\text{ex}} = 480$ nm), and (d) 10 ($\lambda_{\text{ex}} = 510$ nm) in different solvents. In order to demonstrate the relative fluorescence intensity, the emission spectra were not normalized. $c = 1.0 \times 10^{-5}$ M, 20 °C.

acetate, dual emission bands were observed. Similar emission profiles were found for 6 (Figure S24a), except that the emission bands are slightly blue-shifted. These emission properties are similar to HBT. Therefore, the emission of 4 and 6 at 530 nm can be assigned to the radiative decay of the excited *cis* keto tautomer, whereas the emission at 420 nm can be assigned to the excited *enol* tautomer.^{1,2} The emission of 11 confirmed these postulations (Figure 3b). With the hydroxyl group alkylated, 11 shows the same emission in both *protic* and *aprotic* solvents, indicating the absence of ESIPT.

The emissions of 7–10 were also studied (see Figure S24 for the emission of 8 and 9). Different from 4 and 6, the emission bands of 7–9 are not sensitive to the switch from aprotic to protic solvents. Thus, we propose that 7–9 do not undergo ESIPT. The lack of the ESIPT effect for 7–9 is interesting. Previously it was proposed that π -conjugation can impart significant effect on ESIPT of the fluorophores, but the evidence is rare.^{19,36} It should be pointed out that the fluorescence emission of unsubstituted Bodipy is not sensitive to the polarity of the solvents (see Figure S24d Supporting Information). Compound 12 shows similar emission (Figure S24e) compared with unsubstituted Bodipy 1.

Previously HBT- or HBO-based chromophores with a large π -conjugation framework were prepared (the extended π -conjugation is on the benzoxazole unit, different from 7–9), which show ESIPT.^{14,37} Furthermore, the keto emission at

beyond 500 nm are solvent-polarity-dependent (Table 1).³⁷ The keto emission show remarkable red-shift from 520 nm (in cyclohexane) to 620 nm (in chloroform) with increasing the solvent polarity. ESIPT for naphthalene fluorophore has been reported recently.¹⁸ Those compounds show very low

Table 1. Photophysical Properties of Compounds 4 and 6–12 in Different Solvents^a

compd	solvents	λ_{abs}^b (nm)	λ_{em}^c (nm)	ϵ^d ($\text{M}^{-1} \text{cm}^{-1}$)	τ_{F}^e (ns)
4	PhCH ₃	349	531	13900	1.65
	CH ₂ Cl ₂	347	529/416	14900	3.59
	THF	347	530	14900	3.46
	EtOAc	346	530/415	14800	4.24
	MeOH	345	467	14700	3.85
	CH ₃ CN	344	464	14700	3.75
	MeCN	344	464	14700	3.75
6	PhCH ₃	335	495	18600	1.30
	CH ₂ Cl ₂	333	493	19200	6.37
	THF	334	434/488	19300	3.58
	EtOAc	332	493	19200	3.91
	MeOH	332	439	18000	4.15
	CH ₃ CN	330	489	18900	3.70
	MeCN	330	489	18900	3.70
7	PhCH ₃	535	584	56800	3.02
	CH ₂ Cl ₂	533	590	56800	1.65
	THF	531	585	58400	1.85
	EtOAc	529	583	58900	1.97
	MeOH	528	587	57700	0.68
	CH ₃ CN	528	594	55600	0.57
	MeCN	528	594	55600	0.57
8	PhCH ₃	535	582	53000	3.12
	CH ₂ Cl ₂	533	587	52900	1.92
	THF	532	584	55800	2.28
	EtOAc	530	580	54900	2.30
	MeOH	528	585	55400	1.09
	CH ₃ CN	528	589	53800	1.07
	MeCN	528	589	53800	1.07
9	PhCH ₃	580	621	40200	2.29
	CH ₂ Cl ₂	574	621	35600	2.07
	THF	574	621	40200	2.11
	EtOAc	571	615	37200	2.20
	MeOH	569	619	34200	0.96
	CH ₃ CN	571	618	33400	0.73
	MeCN	571	618	33400	0.73
10	PhCH ₃	536	581	40900	3.40
	CH ₂ Cl ₂	534	584	44800	1.93
	THF	532	584	44000	2.29
	EtOAc	531	582	43700	2.42
	MeOH	529	580	42900	1.34
	CH ₃ CN	528	588	43300	1.18
	MeCN	528	588	43300	1.18
11	PhCH ₃	333	374	17800	<i>f</i>
	CH ₂ Cl ₂	332	376	17500	
	THF	333	373	17900	
	EtOAc	331	372	18000	
	MeOH	332	382	22400	
	CH ₃ CN	332	377	20000	
	MeCN	332	377	20000	
12	PhCH ₃	537	569	58300	4.28
	CH ₂ Cl ₂	533	571	57400	3.69
	THF	532	568	57400	3.94
	EtOAc	530	566	57700	3.97
	MeOH	528	568	56500	2.91
	CH ₃ CN	526	569	57000	2.97
	MeCN	526	569	57000	2.97

^aThe excitation wavelength for 4, 6, 11, 7–10, and 12 were 370, 360, 320, 480, 490, 490, 510, and 490 nm, respectively. 1.0×10^{-5} M, 20 °C. ^bAbsorption wavelength. ^cFluorescence emission wavelength. ^dMolar extinction coefficient. ^eFluorescence lifetimes. ^fNot determined.

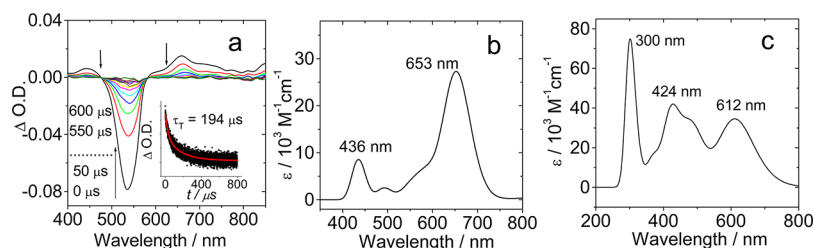


Figure 4. Nanosecond time-resolved transient difference absorption spectra of **7** after pulsed laser excitation ($\lambda_{\text{ex}} = 532 \text{ nm}$) in deaerated toluene. $c = 2.0 \times 10^{-5} \text{ M}$; 20°C . (a) Transient absorption spectra. Inset: decay trace at 550 nm. (b) Calculated absorption spectrum of the triplet excited state of **7**. (c) Calculated absorption spectrum of the putative *trans* keto form of **7**. Toluene was used as solvent in the DFT calculations. Note the bleaching cannot be predicted by the calculations. Calculated at the DFT//B3LYP/6-31G(d) level with Gaussian 09W.

fluorescence quantum yields and large Stokes shift, which are typical for ESIPT chromophores.¹⁸ The absence of ESIPT for **7–9** supported the recent report that the ESIPT can be eliminated by π -conjugation variations.¹⁹

2.4. Nanosecond Time-resolved Transient Difference Absorption Spectra. Time-resolved spectroscopy was used for study of transient species of ESIPT dyes upon photoexcitation.^{12,18} For some compounds, triplet excited state was observed,¹⁸ and in other cases the keto forms were observed; both show slow decay kinetics.¹⁸ The nanosecond time-resolved TA spectroscopy was used to study the possible population of the triplet excited state of the new compounds (Figure 4).

Upon pulsed 532 nm laser excitation, bleaching at 535 nm was observed for **7** (Figure 4a), which indicates depletion of the ground state. TA bands at the 415–480 nm and 584–800 nm range were observed. The significant bleaching is drastically different from the normal ESIPT chromophores.¹⁸ Fitting of the decay of the bleaching at 550 nm gives the lifetime of the transient species as 194 μs . Under aerated condition, however, this transient was significantly quenched ($\tau_{\text{T}} = 0.32 \mu\text{s}$; Figure S26a). On the basis of these results, we propose that the transient species observed are due to the triplet excited state of **7**, not the keto tautomers.¹⁸ Furthermore, the Bodipy unit in **7** contributes significantly to the T_1 excited state, indicated by the remarkable bleaching at 535 nm. This observation is different from that of the HBT. Previously it was shown that the transient species of HBT is due to the keto tautomers, not the triplet excited state.¹⁷

In order to prove the transient of **7** is due to the triplet excited state and not the keto tautomers, the TA of the triplet excited state of **7** was calculated (Figure 4b). The calculated TA bands are located at 436 and 653 nm, which are in good agreement with the experimental results at 441 and 658 nm (Figure 4a). Furthermore, the absorption of the putative keto form of **7** was also calculated (Figure 4c), which is substantially different from the experimental results (Figure 4a). Thus, the transient absorption observed for **7** is due to its triplet excited states. Similar transient signals were observed for **8** (see Figure S28). The triplet excited state lifetime of **8** was determined as 195 μs . The transient can be significantly quenched by O_2 ($\tau = 0.33 \mu\text{s}$ in aerated solution).

Population of the triplet excited states of organic chromophores are important, especially for those showing intense absorption of visible light.^{24,25a,b,33,34,38–43} Previously population of the triplet excited states were observed for naphthalene-derived ESIPT chromophores,¹⁸ but the absorptions of the compounds were in the UV range ($<378 \text{ nm}$) and the triplet excited state lifetimes are much shorter ($\tau_{\text{T}} = 1.4 \mu\text{s}$)

than that of **7**. Absorption in the UV range and a short triplet excited state lifetime are detrimental for the potential applications of the compounds.⁴² Previously, a much shorter triplet excited state lifetime was found for the unsubstituted HBO ($\tau_{\text{T}} = 10.9 \mu\text{s}$).¹⁰ In another study the TA spectra of HBO gives a lifetime of 2.5 μs , which cannot be quenched by O_2 . Thus the transient of HBO is attributed to the ESIPT produced keto form, not the triplet excited state.¹⁶ Our results show that by attaching the HBO moiety to the Bodipy chromophore, the triplet excited state lifetime is greatly extended. No significant TA was observed for the unsubstituted Bodipy. On the other hand, observation of the triplet excited state of the Bodipy chromophore is rare. Previously the triplet excited states of Bodipy were observed with heavy atom effect of iodine^{21,23a,24a,b} and Pt(II) atoms.^{24c} Very few heavy-atom-free Bodipy chromophores were reported to show the triplet excited states populated.^{24d,25a}

TA spectra of **9** were also studied (Figure 5). Significant bleaching at 560 nm and TA bands at 450 nm and in the range

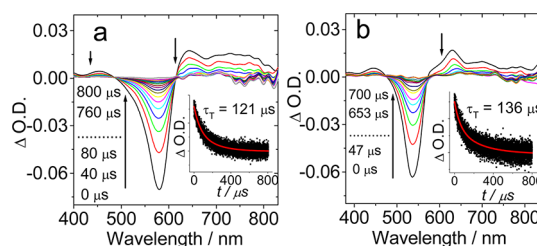


Figure 5. Nanosecond time-resolved transient difference absorption of **9** and **10** after pulsed laser excitation ($\lambda_{\text{ex}} = 532 \text{ nm}$). (a) Transient absorption of **9** and decay trace at 570 nm (inset). (b) Transient absorption of **10** and decay trace at 550 nm (inset). In deaerated toluene. $c = 2.0 \times 10^{-5} \text{ M}$; 20°C .

of 620–800 nm were observed. The lifetime of the transient species determined by following the bleaching at 570 nm is 121 μs . In aerated solution, the lifetime was greatly reduced to 0.51 μs (Figure S26b). Thus the transient species observed were attributed to the triplet excited states.¹⁸ Similar to **7** and **8**, the bleaching of **9** is related to the depletion of the ground state of the Bodipy chromophore.

Upon pulsed laser excitation, significant bleaching at 536 nm was observed for **10** (Figure 5b). Concurrently, TA bands at 405–470 nm and 580–800 nm were observed (Figure 5b). These transients are sensitive to O_2 ($\tau_{\text{T}} = 0.31 \mu\text{s}$ in aerated solution. Figure S26c), and thus the transients are due to triplet excited state, not the keto tautomers,¹⁸ which was confirmed by the calculated TA spectrum. DFT calculations predict transient absorptions at 436 and 658 nm (Figure S29b), which are in

good agreement with the experimental results at 445 and 630 nm (Figure 5b). Since the ESIPT is completely prohibited, thus the population of the triplet excited state of **10** is not due to ESIPT and formation of keto tautomer. This conclusion is different from previous studies.^{12,18}

We noticed that the lifetimes of the triplet excited states of **7–10** are significantly longer than the triplet excited state observed for a ESIPT chromophore (72 μs , 180 K).¹² Previously naphthalene derivatized ESIPT dyes were reported.¹⁸ The nanosecond transient difference absorption spectra show that the chromophores undergo ESIPT upon photoexcitation, that is, keto form was produced. Transient of the keto form (which is not sensitive to O_2) and the triplet excited state was observed (which can be quenched by O_2).¹⁸ However, the lifetime of the triplet excited state is much shorter ($\tau_T < 2.0 \mu\text{s}$) than that of **7–10**.

The TA of **4** is drastically different from that of **7** (Figure 6). For example, the bleaching of **4** is at 350 nm, with transients at

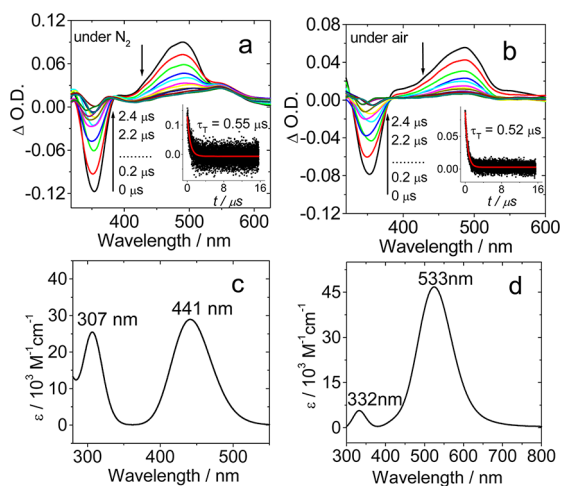


Figure 6. Nanosecond time-resolved transient difference absorption of **4** after pulsed laser excitation ($\lambda_{\text{ex}} = 355 \text{ nm}$). (a) Transient absorption with different delay times. (b) Transient absorption with different delay times. In aerated toluene. $2.0 \times 10^{-5} \text{ M}$; 20°C . Calculated UV-vis absorption of the (c) *cis* keto tautomer and (d) the triplet excited state of **4**. Toluene was used as solvent in the calculations. Calculated at the B3LYP/6-31G(d) level with Gaussian 09W.

488 nm. Furthermore, a short lifetime of $0.55 \mu\text{s}$ was observed. The transient lifetime is $0.52 \mu\text{s}$ in aerated solution (Figure 6b). The large Stokes shift of **4** (ca. 180 nm) and the low fluorescence quantum yields (Table 2) propose that ESIPT exists for **4**, which is similar to that of HBT. In addition, the DFT calculation predicted absorption of keto form of **4** at 441 nm (experimental result is at 488 nm, Figure 6c). The calculated absorption of the triplet excited state (Figure 6d) is not in agreement with the experimental results.

Extension of the π -conjugation framework of **4** changes its photophysical property completely. For example, **7** does not show the ESIPT effect, but the triplet excited state of **7** was populated upon photoexcitation. These properties are in stark contrast to HBT or **4**. No TA signals were observed for **6** either in deaerated solution or in aerated solution. The lack of transient signal of **6** is due to the absence of the triplet excited state and the *trans* keto tautomer.

Compound **11** was also studied (Figure S27). Triplet excited state was populated for **11** upon photoexcitation, and the

Table 2. Photophysical Properties of Compounds **4** and **6–11**

compounds	Φ_F^a	τ_T^b (μs)	τ_T^c (μs)
4	0.002	0.55	0.52
6	0.027		
7	0.225	194	0.32
8	0.202	195	0.33
9	0.360	121	0.51
10	0.223	136	0.31
11	0.111	34.1	0.36

^aFluorescence quantum yields in THF, with compound **1** as the standard ($\Phi = 0.720$ in THF). $1.0 \times 10^{-5} \text{ M}$, 20°C . ^bTriplet state lifetimes, $1.0 \times 10^{-5} \text{ M}$ in deaerated toluene. ^cTriplet state lifetimes, $2.0 \times 10^{-5} \text{ M}$ in air-saturated toluene. ($\lambda_{\text{ex}} = 532 \text{ nm}$). Compound **6** showed no signal in transient absorption.

lifetime of the triplet state was determined as $34.1 \mu\text{s}$ in deaerated solution, which is significantly reduced to $0.36 \mu\text{s}$ in aerated solution. DFT calculation predicted transient absorption at 422 nm, which is in good agreement with the experimental results at 426 nm (Figure S27). Thus the production of the triplet excited state of the compounds described in this paper is not related to ESIPT process.

To the best of our knowledge, the triplet excited state lifetime of the derivatives are the longest observed for Bodipy derivatives. Previously triplet excited state lifetime of 66.3–123.2 μs were observed for Bodipy derivatives,^{24,43h} and herein the lifetime was extended to 136–95 μs (Table 2).

The emission of compound **7** at 77 K was studied (Figure S32). Compared to the emission at room temperature, a new emission band at 630 nm was observed, which is tentatively assigned to the phosphorescence of **7**. Unfortunately the emission is too weak for accurate determination of the lifetime. However, the closely lying S_1 and T_1 states may account for the population of the triplet excited state of compound **7**.

2.5. Spin Density of the Triplet States of the Compounds. In order to study the triplet excited state of the compounds from a theoretical perspective, the spin density surfaces were analyzed by DFT calculations (Figure 7).^{24,41,43}

For **7–10**, the spin density surfaces are localized on the Bodipy moieties. The HBT or the HBO subunits contribute very little to the spin density (Figure 7). This result is in agreement with the nanosecond time-resolved transient difference absorption spectra of these compounds (Figures

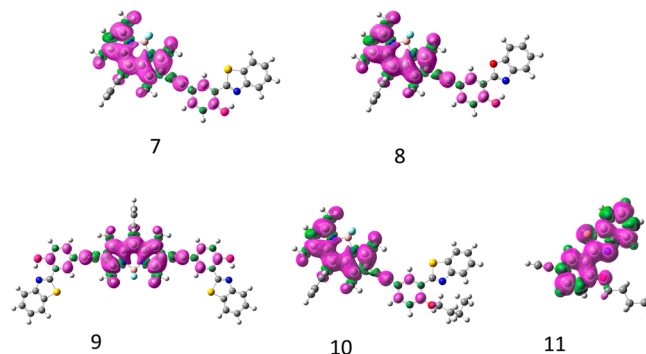


Figure 7. Isosurfaces of spin density of compounds **7–11** at the optimized triplet state geometries. Toluene was used as solvent in the calculations. Calculation was performed at the B3LYP/6-31G(d) level with Gaussian 09W.

3–6). Furthermore, the bleaching observed in the transient absorption spectra of 7–9 is due to the depletion of the ground state of the Bodipy units, which is supported by the spin density distributions (Figure 7).

The spin density surface of **11** is localized in the benzothiazole moiety, which is drastically different from the spin density surfaces of 7–10. The nanosecond time-resolved transient difference absorption spectrum of **11** (Figure S27) is drastically different from that of 7–10. Thus our assignment of the Bodipy moiety localized triplet excited states for 7–10 is fully supported by the spin density analysis of these compounds and the control compound **11**.

2.6. DFT Calculations on the UV–vis Absorption and Fluorescence Emission. Recently DFT calculations have been used for study of photophysical properties of fluorophores.^{44–51} Previously we proposed to use the concept of “electronic state”, rather than the conventional approximation of “molecular orbitals”, to study the emission of fluorescent molecular probes.^{46a,47} We also used the concept of “dark state” to rationalize the fluorescence OFF–ON switching effect of thiol probes,⁴⁷ as well as the d-PET mechanism of the boronic acid molecular probes.⁴⁶

The ground state geometry of **7** was optimized (Figure 8). The Bodipy and HBT moiety take coplanar geometry and thus

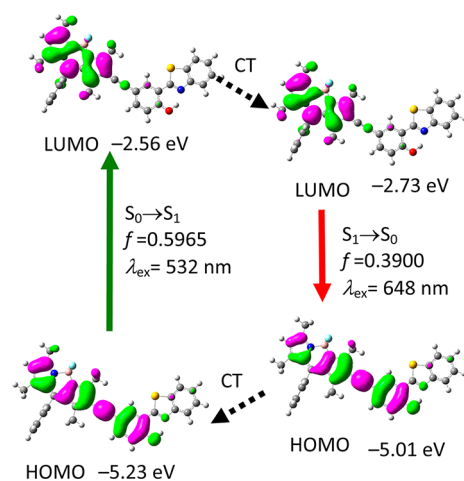


Figure 8. Selected frontier molecular orbitals involved in the excitation and emission of compound **7**. CT stands for conformation transformation. The calculations are based on the optimized ground state geometry (S_0 state, for the excitation) and excited state geometry (S_1 state, for the emission) at the B3LYP/6-31G(d)/ level using Gaussian 09W.

ensure a full π -conjugation between the two units. On the basis of the optimized ground state geometry, the UV–vis absorption of **7** was calculated by TDDFT (Franck–Condon principle, Table 3). The calculated excitation wavelength for the $S_0 \rightarrow S_1$ transition is 532 nm, which is very close to the experimental result (535 nm, Figure 1). HOMO is distributed on the Bodipy-ethynylphenyl moiety, whereas the LUMO is localized on Bodipy unit. The benzothiazole moiety, especially the N atom, is not involved in HOMO and LUMO. As a result, the basicity of the N atom in the benzothiazole moiety does not increase upon photoexcitation. Thus, the absence of benzothiazole moiety in the frontier molecular orbitals may be responsible for the lack of ES IPT of **7**.^{19,52}

The geometry of the S_1 state of **7** was optimized, and the fluorescence wavelength was calculated based on the optimized

Table 3. Selected Electronic Excitation Energies (eV) and Corresponding Oscillator Strengths (f), Main Configurations, and CI Coefficients of the Low-Lying Electronically Excited States of Compound **7**^a

electronic transition	TDDFT//B3LYP/6-31G(d)			
	energy ^b	f^c	composition ^d	CI ^e
$S_0 \rightarrow S_1$	2.33 eV/532 nm	0.5965	H→L	0.6935
			H-1→L	0.1176
$S_0 \rightarrow S_3$	3.02 eV/410 nm	0.5503	H→L	0.1227
			H-1→L	0.6746
			H→L+1	0.1516
$S_0 \rightarrow S_6$	3.65 eV/340 nm	0.2027	H-1→L+1	0.6827
			H→L+2	0.1011
$S_0 \rightarrow S_{11}$	3.99 eV/311 nm	0.8755	H-5→L	0.2234
			H-2→L+1	0.4165
			H-1→L+1	0.1156
			H→L+2	0.4775
$S_1 \rightarrow S_0$	1.91 eV/648 nm	0.3900	H→L	0.7014

^aCalculated by TDDFT//B3LYP/6-31G(d), based on the DFT//B3LYP/6-31G(d) optimized ground state geometries. ^bOnly the low-lying excited states and some allowed transitions are presented. ^cOscillator strength. ^dH stands for HOMO, and L stands for LUMO. Only the main configurations are presented. ^eCI coefficients are in absolute values.

S_1 state geometry (Figure 8). For most fluorophores, S_1 excited state is involved in fluorescence (Kasha’s rule).⁵³ With optimization of the S_1 state geometry, the energy level of the LUMO decreased from -2.56 to -2.73 eV. Conversely, the energy level of HOMO promoted from -5.23 to -5.01 eV. The calculated emission at 648 nm is reasonably close to the experimental results of 584 nm (Figure 1). The DFT calculations indicate that the benzothiazole moiety is not involved in the frontier molecular orbitals of the absorption and emission transitions, which can be used to rationalize the lack of ES IPT effect for the dyes.¹⁹

The same theoretical calculations were applied to **4**, which was proved to undergo ES IPT. The electron density on the hydroxyl group decreased, whereas the electron density on the N atom of benzothiazole moiety increased upon photoexcitation (Figure 9). This electron density change indicates that both the acidity of the hydroxyl group and the basicity of N atom will increase upon excitation, which coincides with the occurrence of ES IPT.¹⁹ The excited states geometries of both the enol and keto of **4** were calculated (Table 4). The emission wavelength of the enol form was calculated as 410 nm, which is in good agreement with the experimental results of 414 nm (Figure 3). The emission of the keto tautomer was calculated as 515 nm, which is close to the experimental results (531 nm, Figure 3).

2.7. Energy Barrier for the Intramolecular Proton Transfer at the Excited State and Ground State. In order to explain the different ES IPT properties of the compounds, the potential energy curves of the intramolecular proton transfer (i.e., the transformation from the enol form to the keto form) at both the ground state and the excited state were studied (Figure 10, Table 5, and Supporting Information). Generally, for the compounds that show the ES IPT effect, there is substantial free energy decrease (ΔE) for the transformation from the enol form to the keto form at the S_1 state (compounds **4** and **6**). Conversely, for the compounds lacking ES IPT, the

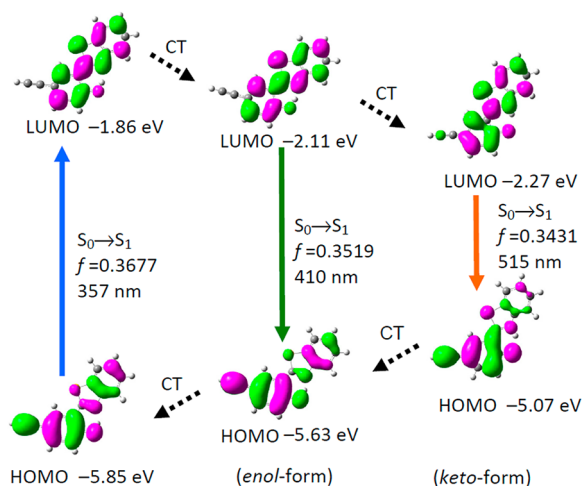


Figure 9. Selected frontier molecular orbitals involved in the vertical excitation and the singlet excited state (S_1) (both enol form and keto form were calculated) of compound 4. CT stands for conformation transformation. The calculations are based on the optimized ground state geometry (S_0 state, excitation) and excited state geometry (S_1 state, emission) at the B3LYP/6-31G(d)/ level using Gaussian 09W.

Table 4. Selected Electronic Excitation Energies (eV) and Corresponding Oscillator Strengths (f), Main Configurations, and CI Coefficients of the Low-Lying Electronically Excited States of Compound 4^a

singlet	electronic transition	TDDFT//B3LYP/6-31G(d)			
		energy ^b	f^c	composition ^d	CI ^e
(UV-vis)	$S_0 \rightarrow S_1$	3.47 eV/357 nm	0.3677	H→L	0.6959
	$S_0 \rightarrow S_2$	4.13 eV/300 nm	0.2553	H→2→L H→1→L	0.3376 0.6000
(FL)-enol	$S_0 \rightarrow S_1$	3.03 eV/410 nm	0.3519	H→L	0.7008
(FL)-keto	$S_0 \rightarrow S_1$	2.41 eV/515 nm	0.3431	H→L	0.7076

^aCalculated by TDDFT//B3LYP/6-31G(d). FL stands for fluorescence. ^bOnly selected low-lying excited states are presented. ^cOscillator strength. ^dH stands for HOMO and L stands for LUMO. Only the main configurations are presented. ^eCI coefficients are in absolute values.

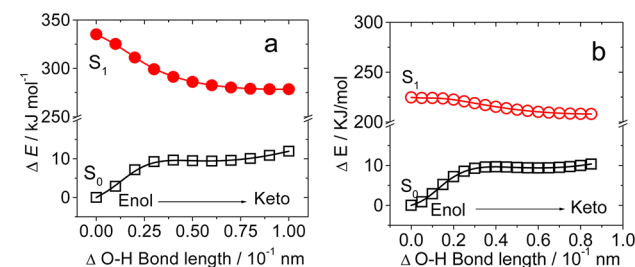


Figure 10. Potential energy curves from enol form to keto form of the compounds 4 (a) and 7 (b) at the excited state and ground state. The calculations are based on the optimized ground state geometry (S_0 state) at the B3LYP/6-31G(d)/ level using Gaussian 09W.

ΔE values are much smaller and are similar to those at ground states (Table 5). For example, the ΔE value of 4 is 9.7 kJ/mol at S_0 state but changes to -52.7 kJ/mol at S_1 state (Figure 10a). This energy changing profile at excited state coincides with the

Table 5. Free Energy Changes for the Transformation from Enol Form to Keto Form of the Compounds at the Excited State and Ground State

compound	ΔE (kJ mol ⁻¹) ^a	ΔE (kJ mol ⁻¹) ^b
4	9.7	-52.7
6	11.6	-52.4
7	9.7	-14.5
8	11.6	-13.5
9	9.3	-6.6

^aAt S_0 (ground state) state. ^bAt S_1 state.

observed ESIPT of 4.⁵⁴ For 7, however, the ΔE value at the ground state and excited states are 9.7 and -14.5 kJ mol⁻¹, respectively (Figure 10b). The small energy decrease of compound 7 at S_1 state indicated that the driving force for the ESIPT of 7 at the S_1 state is smaller than that of compound 4. Similar ΔE value profiles were found for the compounds that do not undergo ESIPT (Table 5 and Figure S31).

2.8. Application of the Long-lived Triplet Excited State and the Visible Light Harvesting Effect: Singlet Oxygen (1O_2) Photosensitizer for Photooxidation. To date most of the triplet photosensitizers are transition metal complexes or porphyrin derivatives.^{23,34,55} Organic triplet photosensitizers (heavy-atom-free) are rarely reported.^{22,24d,25a,34,39,53} Since 7–10 show intense absorption of visible light ($\epsilon = 50000$ M⁻¹ cm⁻¹ at 530–580 nm) and long-lived triplet excited states ($\tau_T > 100$ μ s at RT), these compounds were used as triplet photosensitizers to initiate photophysical processes.

Herein as a proof-of-concept, compounds 7–10, in which no heavy atoms are presented (Scheme 1), were used as singlet O_2 (1O_2) photosensitizer for photooxidation with 1,5-dihydroxynaphthalene (DHN) as the substrate, to produce juglone (Scheme 2).²⁶ Previously Ir(III) complex ([Ir(ppy)₂(phen)]-[PF₆]) was successfully used as 1O_2 sensitizer for photooxidation of DHN.²⁶ However, the conventional Ir(III) complexes show very weak absorption of visible light.⁵⁶ Furthermore, these transition metal complex triplet sensitizers are not cost-efficient. Organic triplet sensitizers are ideal alternatives to replace these expensive transition metal complex triplet photosensitizers.

The principle of the photooxidation of DHN is outlined in Scheme 2.²⁶ Upon photoexcitation of the triplet photosensitizers, the singlet excited state of the sensitizers was first populated (e.g., $S_0 \rightarrow S_1$). Then with ISC effect, the triplet excited states (e.g., T_1) of the sensitizers are populated. Collision between the sensitizers at the triplet excited state with the O_2 molecules (for which the ground state is the triplet state, 3O_2) imparts triplet–triplet energy transfer (TTET), and thus singlet 1O_2 was produced. DHN is oxidized by 1O_2 to give an intermediate peroxide and then to produce the final product of juglone. The progress of photooxidation of DHN can be followed by the decreasing of the UV-vis absorption at 301 nm.²⁶

Compounds 7–10 were used as 1O_2 photosensitizer for photooxidation of DHN (Figure 11). The performance of these organic sensitizers was compared with the model triplet photosensitizer ([Ir(ppy)₂(phen)]-[PF₆]) (Ir-1). For 8 (Figure S33a), the UV-vis absorption of the sensitizer/DHN solution upon photoirradiation does not change significantly. For 9, however, the change is more remarkable, with decreased absorption at 301 nm and the development of the new

Scheme 2. Mechanism for the Photooxidation of DHN with a Triplet Photosensitizer; BDP = Bodipy Compounds

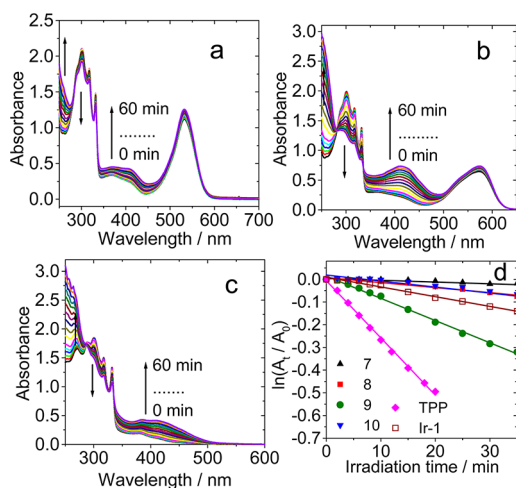
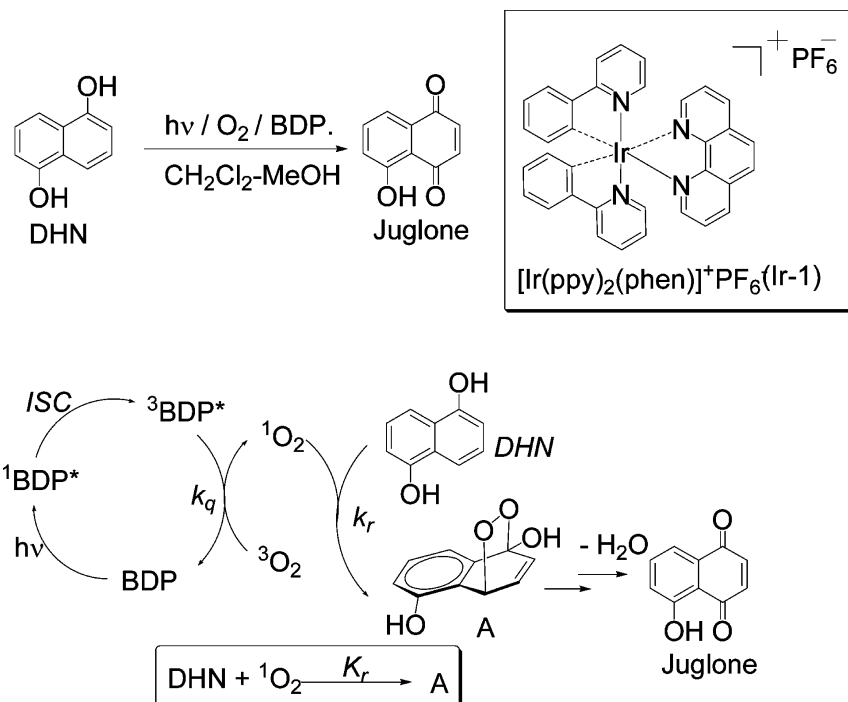


Figure 11. Absorption spectra for the photooxidation of DHN using the BODIPY derivatives as the triplet sensitizers. Compounds (a) 7, (b) 9, and (c) Ir-1. (d) Plots of $\ln(A_t/A_0)$ vs irradiation time (t) for the photooxidation of DHN with different triplet photosensitizers. c [sensitizers] = 2.0×10^{-5} M, c [DHN] = 2.0×10^{-4} M, in CH₂Cl₂/MeOH (9:1, v/v), 20 °C.

absorption band of juglone at 427 nm. Similar changes were observed with Ir-1 (Figure 11c). The UV-vis absorption of these organic triplet photosensitizers are much red-shifted compared to that of the model Ir(III) complexes.²⁶

The performance of the sensitizers can be quantified by plotting the absorption variation ($\ln(A_t/A_0)$) against the irradiation time (Figure 11d). It is clear that 9 is the most efficient triplet photosensitizer. The rate constant k_{obs} is $9.8 \times 10^{-3} \text{ min}^{-1}$, which is more than 2-fold that of Ir-1 ($k_{obs} = 4.3 \times 10^{-3} \text{ min}^{-1}$). Ir-1 was used as ¹O₂ photosensitizer for photooxidation of DHN (Table 6).²⁶ Thus our results show that organic triplet photosensitizers could be more efficient than the traditional transition metal complexes. We propose

Table 6. Pseudo-first-order Kinetics Parameters for Compounds 7–10 and the Control Compounds Ir-1 and TPP

compound	k_{obs} (min ⁻¹) ^a	ν_i ^b	yield (%) ^c
7	0.8	1.6	18.1
8	2.2	4.4	0.2
9	9.8	19.6	59.2
10	2.6	5.2	25.8
Ir-1	4.3	8.6	33.5
TPP	25.2	50.4	89.1

^aPseudo-first-order rate constant k_{obs} was calculated by the rule: $\ln(C_t/C_0) = -k_{obs}t$. In 10^{-3} min^{-1} . ^bInitial consumption rate of DHN, $\nu_i = k_{obs}[\text{DHN}]$. In $10^{-7} \text{ M min}^{-1}$. ^cYield of juglone after reaction for 50 min.

that the efficient ¹O₂ production with 9 may be due to its efficient ISC property. Two benzothiazole units exist in this compound, which is different from other compounds. The performance of the organic triplet sensitizers was compared with *meso*-tetraphenylporphine (TPP, Figure 11d; see Figure S33c for the results of TPP).⁵⁷ We found that the performance of 9 is close to TPP. The yield of juglone against the irradiation time was also studied (Figure 12).

2.9. Conclusions. In summary, new Bodipy fluorophores conjugated with 2-(2-hydroxyphenyl) benzothiazole (HBT)/benzoxazole (HBO) units were prepared, with the intention to access ES IPT compounds that give red-shifted absorption compared to the conventional ES IPT chromophores such as HBT and HBO, which show absorption in the UV or blue range. The new compounds show much red-shifted absorption (530–580 nm) compared to HBT and HBO (ca. 350 nm). Interestingly, the new compounds show small Stokes shifts (45 nm) and high fluorescence quantum yields ($\Phi_F > 20\%$), which are in stark contrast to the typical features of the conventional ES IPT dyes (Stokes shift > 100 nm and $\Phi_F < 1\%$). By comparison with the compounds that with the hydroxyl group

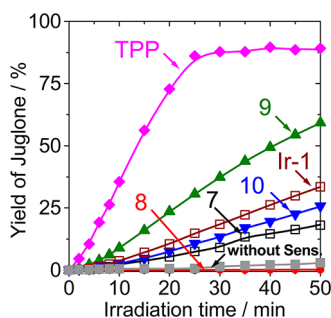


Figure 12. Plots of chemical yield as a function of irradiation time for the photooxidation of DHN using 7–10, Ir-1, and TPP as sensitizers. Blank experiment without any sensitizer is also presented (without sens.). c [sensitizers] = 2.0×10^{-5} M, c [DHN] = 2.0×10^{-4} M, in $\text{CH}_2\text{Cl}_2/\text{MeOH}$ (9:1, v/v), 20 °C.

alkylated, we propose that the new fluorophores *do not* undergo ESIPT upon photoexcitation. Nanosecond time-resolved transient difference absorption spectroscopy demonstrated that long-lived triplet excited states (τ_T is up to 195 μs) were populated for the dyes 7–9 upon photoexcitation, as well as for those with the hydroxyl groups alkylated (10, ESIPT is completely prohibited). This result is different from a previous report that the triplet excited state is the result of ESIPT. The triplet excited states are localized on the Bodipy moiety, proved by the time-resolved transient absorption spectra and the spin density analysis of the triplet states. The compounds were used as organic triplet photosensitizers for production of singlet oxygen ($^1\text{O}_2$), demonstrated with the photooxidation of 1,5-dihydroxynaphthalene (DHN). One of the dyes is 2-fold more efficient for photooxidation than the conventional Ir(III) complex triplet sensitizer ($[\text{Ir}(\text{ppy})_2(\text{phen})][\text{PF}_6]_2$). Our result will be useful for design of new ESIPT compounds, as well as organic triplet photosensitizers that show the *predetermined* intersystem crossing (ISC) ability and for their applications in photovoltaics, photocatalysis and upconversions, etc.

3. EXPERIMENTAL SECTION

3.1. General Methods. Fluorescence lifetimes were measured with a OB920 phosphorescence/fluorescence lifetime spectrometer (Edinburgh Instruments, U.K.). Nanosecond time-resolved transient difference absorption spectra were measured with a LP920 Laser Flash Photolysis Spectrometer (Edinburgh Instruments, U.K.), and the data were recorded on a Tektronix TDS 3012B oscilloscope. The lifetime values (by monitoring the decay trace of the transients) were obtained with the LP900 software.

3.2. 1,3,5,7-Tetramethyl-8-phenyl-4,4-difluoroboradiazaindacene (1).^{58a} 2-iodo-1,3,5,7-tetramethyl-8-phenyl-4,4-difluoroboradiazaindacene (2a),²⁴ 2,6-diiodo-1,3,5,7-tetramethyl-8-phenyl-4,4-difluoroboradiazaindacene (2b),^{58a} 5-ethynyl-2-hydroxybenzaldehyde (3),^{58b} and 2-benzoxazol-2-yl-4-bromo-phenol (5)^{58c} were synthesized according to literature methods.

3.3. 2-(5'-Ethynyl-2'-hydroxyphenyl)benzothiazole (4). A mixture of 3 (300.0 mg, 2.1 mmol), 2-aminothiophenol (500.0 mg, 4.0 mmol), and methanol (20 mL) was stirred at room temperature (rt) for 12 h. After removal of the solvent under reduced pressure, the residue was purified with column chromatography (silica gel, $\text{CH}_2\text{Cl}_2/\text{petroleum ether}$, 1:1, v/v) to give 155.0 mg of a white powder. Yield: 30%. Mp 143.7–144.6 °C. ^1H NMR (400 MHz, CDCl_3) δ 8.02 (d, 1H, $J = 8.4$ Hz), 7.95 (d, 1H, $J = 8.0$ Hz), 7.87 (s, 1H), 7.43–7.55 (m, 3H), 7.08 (d, 1H, $J = 8.4$ Hz), 3.07 (s, 1H). ^{13}C NMR (100 MHz, CDCl_3) δ 168.4, 158.5, 152.0, 136.3, 132.7, 132.4, 127.0, 126.0, 122.4, 121.7, 118.4, 116.9, 113.3, 83.0, 76.5. TOF HRMS EI^+ : calcd $[\text{C}_{15}\text{H}_9\text{NOS}]^+$ m/z 251.0405, found m/z 251.0408.

3.4. 2-(5'-Ethynyl-2'-butoxyphenyl)benzothiazole (11). A mixture of 4 (200.0 mg, 0.8 mmol), K_2CO_3 (200.0 mg, 1.4 mmol), and dimethyl formamide (1 mL) was stirred at rt for 10 min, and then *n*-butyl bromide (0.4 mL, 3.7 mmol) was added. The mixture was stirred at 50 °C for 4 h and then poured into 300 mL of ice–water mixture. The product was extracted with CH_2Cl_2 (9 \times 30 mL), and the organic layers were dried over Na_2SO_4 . After removal of solvent under reduced pressure, the residue was purified with column chromatography (silica gel, $\text{CH}_2\text{Cl}_2/\text{petroleum ether}$, 1:1, v/v) to give 211.0 mg (yield 86%) of a white powder. Mp 134.2–135.4 °C. ^1H NMR (400 MHz, CDCl_3) δ 8.73 (s, 1H), 8.11 (d, 1H, $J = 8.0$ Hz), 7.95 (d, 1H, $J = 8.0$ Hz), 7.56 (d, 1H, $J = 8.8$ Hz), 7.52 (t, 1H, $J = 7.2$ Hz), 7.40 (t, 1H, $J = 7.2$ Hz), 7.00 (d, 1H, $J = 8.8$ Hz), 4.24–4.21 (m, 2H), 3.04 (s, 1H), 1.99–2.04 (m, 2H), 1.61–1.66 (m, 2H), 1.06 (t, 3H, $J = 7.2$ Hz). ^{13}C NMR (100 MHz, CDCl_3) δ 162.2, 157.0, 152.1, 136.3, 135.4, 133.6, 126.2, 125.0, 123.0, 122.4, 121.4, 114.9, 112.3, 83.1, 76.6, 69.4, 31.3, 19.7, 14.1. TOF HRMS EI^+ : calcd $[\text{C}_{19}\text{H}_{17}\text{NOS}]^+$ m/z 307.1031, found m/z 307.1031.

3.5. 2-(5'-Ethynyl-2'-hydroxyphenyl)benzoxazol (6). Under Ar atmosphere, compound 5 (120.0 mg, 0.4 mmol), $\text{PdCl}_2(\text{PPh}_3)_2$ (8.4 mg, 0.012 mmol), PPh_3 (5.2 mg, 0.02 mmol), and CuI (3.8 mg 0.02 mmol) were dissolved in triethylamine (12 mL). After stirring, ethynyltrimethylsilane (1.5 mL, 0.69 mmol) was added via syringe. The solution was stirred at 80 °C for 4 h. After removal of solvent under reduced pressure, the residue was purified with column chromatography (silica gel, $\text{CH}_2\text{Cl}_2/\text{petroleum ether}$, 1:1, v/v) to give 89.0 mg (yield 70%) of a white powder. Then the mixture of the white powder (89.0 mg, 0.3 mmol), K_2CO_3 (800.0 mg, 6 mmol), CH_2Cl_2 (3 mL), and CH_3OH (7 mL) was stirred at rt for 6 h. The yellow solution was washed with water. The aqueous phase was extracted with CH_2Cl_2 . After removal of solvent under reduced pressure, the residue was purified with column chromatography (silica gel, $\text{CH}_2\text{Cl}_2/\text{petroleum ether}$, 1:1, v/v) to give 34.0 mg (yield 50%) of white powder. The overall yield was 35.0%. Mp 144.6–145.7 °C. ^1H NMR (400 MHz, CDCl_3) δ 8.20 (s, 1H), 7.75 (d, 1H, $J = 5.6$ Hz), 7.62 (d, 1H, $J = 5.2$ Hz), 7.56 (d, 1H, $J = 8.4$ Hz), 7.39–7.42 (m, 2H), 7.09 (d, 1H, $J = 8.8$ Hz), 3.05 (s, 1H). ^{13}C NMR (100 MHz, CDCl_3) δ 162.1, 159.1, 149.2, 139.9, 137.1, 136.3, 131.2, 129.5, 126.0, 125.3, 119.6, 117.9, 113.6, 82.9, 76.4. TOF HRMS EI^+ : calcd $[\text{C}_{15}\text{H}_9\text{NO}_2]^+$ m/z 235.0633, found m/z 235.0637.

3.6. Compound 7. Under Ar atmosphere, compound 2a (80.0 mg, 0.18 mmol), 4 (45.0 mg, 0.18 mmol), $\text{Pd}(\text{PPh}_3)_4$ (20.8 mg, 0.018 mmol), and CuI (1.7 mg 0.01 mmol) were dissolved in triethylamine (2 mL) and THF (10 mL). The solution was stirred at 60 °C for 6 h. After removal of solvent under reduced pressure, the residue was purified with column chromatography (silica gel, $\text{CH}_2\text{Cl}_2/n$ -hexane, 1:1, v/v) to give 41.0 mg (yield 40%) of a dark red powder. Mp > 250 °C. ^1H NMR (400 MHz, CDCl_3) δ 8.01 (d, 1H, $J = 8.0$ Hz), 7.93 (d, 1H, $J = 8.0$ Hz), 7.79 (s, 1H), 7.51–7.54 (m, 4H), 7.43–7.47 (m, 2H), 7.29–7.31 (m, 2H), 7.07 (d, 1H, $J = 8$ Hz), 6.04 (s, 1H), 2.73 (s, 3H), 2.59 (s, 3H), 1.54 (s, 3H), 1.41 (s, 3H). ^{13}C NMR (100 MHz, CDCl_3) δ 168.7, 158.0, 157.8, 156.7, 151.8, 144.9, 142.8, 142.2, 135.8, 134.9, 132.8, 132.6, 131.3, 130.5, 129.4, 128.1, 127.0, 126.0, 122.4, 122.3, 121.8, 118.4, 117.0, 115.3, 115.0, 95.0, 81.2, 14.9, 14.7, 13.8, 13.4. TOF HRMS ES^+ : calcd $[\text{C}_{34}\text{H}_{26}\text{BF}_2\text{N}_3\text{OS} + \text{H}]^+$ m/z 574.1936, found m/z 574.1943.

3.7. Compound 8. Under Ar atmosphere, compound 2a (75.0 mg, 0.17 mmol), compound 6 (45.0 mg, 0.19 mmol), $\text{Pd}(\text{PPh}_3)_4$ (19.6 mg, 0.017 mmol), and CuI (1.7 mg 0.01 mmol) were dissolved in triethylamine (2 mL) and THF (10 mL). The solution was stirred at 60 °C for 6 h. After removal of the solvent under reduced pressure, the residue was purified with column chromatography (silica gel, $\text{CH}_2\text{Cl}_2/n$ -hexane, 1:1, v/v) to give 9.5 mg (yield 10%) of a dark red powder. Mp > 250 °C. ^1H NMR (400 MHz, CDCl_3) δ 8.13 (s, 1H), 7.75 (d, 1H, $J = 5.6$ Hz), 7.63 (d, 1H, $J = 3.6$ Hz), 7.50–7.52 (m, 4H), 7.39–7.41 (m, 2H), 7.29–7.31 (m, 2H), 7.09 (d, 1H, $J = 8.4$ Hz), 6.04 (s, 1H), 2.73 (s, 3H), 2.59 (s, 3H), 1.53 (s, 3H), 1.41 (s, 3H). ^{13}C NMR (100 MHz, CDCl_3) δ 162.3, 158.6, 157.8, 156.7, 149.4, 144.8, 142.8, 142.2, 140.0, 136.6, 134.9, 130.1, 129.4, 128.1, 125.9, 125.4, 122.3,

120.0, 118.0, 115.2, 110.0, 95.1, 81.2, 15.0, 14.7, 13.8, 13.4. ESI-HRMS LD⁺: calcd [C₃₄H₂₆BF₂N₃O₂]⁺ *m/z* 557.2086, found *m/z* 557.2119.

3.8. Compound 9. Under Ar atmosphere, compound **2b** (40.0 mg, 0.07 mmol), **4** (70.0 mg, 0.28 mmol), Pd(PPh₃)₄ (8.1 mg, 0.007 mmol), and CuI (0.8 mg, 0.004 mmol) were dissolved in triethylamine (3.0 mL) and THF (10 mL). The solution was stirred at 60 °C for 8 h. After removal of solvent under reduced pressure, the residue was purified with column chromatography (silica gel, CH₂Cl₂/*n*-hexane, 1:1, v/v) to give 14.4 mg (yield 25%) of a dark red powder. Mp > 250 °C. ¹H NMR (400 MHz, CDCl₃) δ 8.02 (d, 2H, *J* = 7.6 Hz), 7.94 (d, 2H, *J* = 7.6 Hz), 7.80 (s, 2H), 7.43–7.56 (m, 9H), 7.32–7.34 (m, 2H), 7.09 (d, 2H, *J* = 7.6 Hz), 2.77 (s, 6H), 1.54 (s, 6H). TOF HRMS LD⁺: calcd [C₄₉H₃₃BF₂N₄O₂S₂]⁺ *m/z* 822.2106, found *m/z* 822.2031.

3.9. Compound 10. Under Ar atmosphere, compound **2a** (30.0 mg, 0.07 mmol), **11** (40.0 mg, 0.13 mmol), PdCl₂(PPh₃)₂ (7.0 mg, 0.01 mmol), PPh₃ (3.0 mg, 0.01 mmol), and CuI (1.9 mg, 0.01 mmol) were dissolved in triethylamine (10 mL). The solution was stirred at 60 °C for 6 h. After removal of solvent under reduced pressure, the residue was purified with column chromatography (silica gel, CH₂Cl₂/*n*-hexane, 1:1, v/v) to give 15.0 mg (yield 36%) of dark red powder. Mp > 250 °C. ¹H NMR (400 MHz, CDCl₃) δ 8.68 (s, 1H), 8.13 (d, 1H, *J* = 8.0 Hz), 7.96 (d, 1H, *J* = 7.6 Hz), 7.49–7.53 (m, 5H), 7.41 (t, 1H, *J* = 7.6 Hz), 7.29–7.31 (m, 2H), 7.02 (d, 1H, *J* = 8.8 Hz), 6.03 (s, 1H), 4.26 (t, 2H, *J* = 6.4 Hz), 2.73 (s, 3H), 2.59 (s, 3H), 2.00–2.03 (m, 2H), 1.61–1.67 (m, 2H), 1.53 (s, 3H), 1.40 (s, 3H), 1.06 (t, 3H, *J* = 7.2 Hz). ¹³C NMR (100 MHz, CDCl₃) δ 162.4, 157.5, 156.9, 156.5, 152.1, 144.6, 136.3, 135.8, 135.4, 134.9, 134.7, 132.5, 130.4, 129.3, 128.1, 126.2, 124.9, 123.0, 122.7, 122.5, 121.4, 116.5, 112.5, 95.4, 81.3, 69.4, 31.4, 19.7, 14.7, 14.1, 13.8, 13.4. TOF HRMS ES⁺: calcd [C₃₈H₃₄BF₂N₃OS+ H]⁺ *m/z* 630.2562, found *m/z* 630.2543.

3.10. Compound 12. Under Ar atmosphere, compound **2a** (31.5 mg, 0.07 mmol), phenylacetylene (21.4 mg, 0.21 mmol), PdCl₂(PPh₃)₂ (7.0 mg, 0.01 mmol), PPh₃ (3.0 mg, 0.01 mmol), and CuI (1.9 mg, 0.01 mmol) were dissolved in triethylamine (10 mL). The solution was stirred at 60 °C for 6 h. After removal of solvent under reduced pressure, the residue was purified with column chromatography (silica gel, CH₂Cl₂/petroleum ether, 1:3, v/v) to give 24.0 mg (yield 81%) of an orange powder. Mp 189.6–191.2 °C. ¹H NMR (400 MHz, CDCl₃) δ 7.51–7.50 (m, 3H), 7.46–7.44 (m, 2H), 7.31–7.28 (m, 5H), 6.03 (s, 1H), 2.70 (s, 3H), 2.58 (s, 3H), 1.50 (s, 3H), 1.40 (s, 3H). ¹³C NMR (100 MHz, CDCl₃) δ 157.7, 156.7, 144.8, 142.9, 142.3, 134.9, 132.6, 130.5, 129.4, 128.5, 128.1, 128.0, 123.8, 122.3, 115.4, 96.0, 82.1, 14.9, 14.7, 13.7, 13.3. TOF HRMS ES⁺: calcd [C₂₇H₂₃BF₂N₂]⁺ *m/z* 424.1922, found *m/z* 424.1921.

3.11. Photooxidation Setup. A 35 W xenon lamp was used for irradiation. NaNO₂ solution (50 g/L) was set between the lamp and the photoreactor to block the <385 nm UV light, as well as the IR light. The irradiation power density at the photoreactor was set at 13 mW/cm². The photosensitizers (2.0 × 10⁻⁵ M) and DHN (2.0 × 10⁻⁴ M) were in CH₂Cl₂/MeOH mixed solvent (9:1). Oxygen (O₂) was bubbled through the solution for 10 min. Then the solution was continuously irradiated by the xenon lamp. The UV–vis absorption of the solutions was measured every 2 min during the first 10 min of the photoreaction. Then the UV–vis absorption of the solution was measured every 5 min.

3.12. DFT Calculations. The geometries of the compounds were optimized using density functional theory (DFT) with B3LYP functional and 6-31G(d) basis set. There are no imaginary frequencies for all optimized structures. Time-dependent DFT (TDDFT) was used for the calculation of the electronic spectra of the compounds. The steady-state UV–vis absorption of the organic dyes was calculated with the optimized S₀ state geometry. The fluorescence of the compounds was calculated with the optimized S₁ state geometry. TDDFT calculations were also used for the prediction of the UV–vis absorption of the organic dyes at triplet state, and in our case it is the transient absorption of the organic dyes after laser flash. Please note that the bleaching bands in the time-resolved transient absorption spectra can be predicted by the TDDFT calculations. The spin density of the compounds were calculated based on the optimized triplet state geometry. The potential energy curves of the ES IPT (the C–H bond

length) was calculated as the singlet point energy at the optimized S₀ state and the vertical excitation energy (S₁ state). The energy shown in the curves are relative values, with the lowest point on the curve as zero. All these calculations were performed with Gaussian 09W.⁵⁹

■ ASSOCIATED CONTENT

📄 Supporting Information

Structural characterization data of the compounds, solvent-dependent fluorescence spectra, nanosecond time-resolved transient difference absorption spectra, and *z*-matrix of the calculated compounds. This material is available free of charge via the Internet at <http://pubs.acs.org>.

■ AUTHOR INFORMATION

✉ Corresponding Author

*E-mail: zhaojzh@dut.edu.cn.

Notes

The authors declare no competing financial interest.

■ ACKNOWLEDGMENTS

We thank the NSFC (20972024 and 21073028), the Royal Society (U.K.) and NSFC (China-UK Cost-Share Science Networks, 21011130154), the Fundamental Research Funds for the Central Universities (DUT10ZD212), Ministry of Education (NCET-08-0077) and Dalian University of Technology for financial support.

■ REFERENCES

- (1) Hsieh, C.; Jiang, C.; Chou, P. *Acc. Chem. Res.* **2010**, *43*, 1364–1374.
- (2) Kwon, J. E.; Park, S. Y. *Adv. Mater.* **2011**, *23*, 3615–3642.
- (3) Zhao, J.; Ji, S.; Chen, Y.; Guo, H.; Yang, P. *Phys. Chem. Chem. Phys.* **2012**, *14*, 8803–8817.
- (4) (a) Wu, J.; Liu, W.; Ge, J.; Zhang, H.; Wang, P. *Chem. Soc. Rev.* **2011**, *40*, 3483–3495. (b) Kim, S. K.; Lee, D. H.; Hong, J.-I.; Yoon, J. *Acc. Chem. Res.* **2009**, *42*, 23–31.
- (5) (a) Wu, Y.; Peng, X.; Fan, J.; Gao, S.; Tian, M.; Zhao, J.; Sun, S. J. *Org. Chem.* **2007**, *72*, 62–70. (b) Xu, Y.; Pang, Y. *Dalton Trans.* **2011**, *40*, 1503–1509. (c) Chen, W.; Xing, Y.; Pang, Y. *Org. Lett.* **2011**, *13*, 1362–1365. (d) Luxami, V.; Kumar, S. *New J. Chem.* **2008**, *32*, 2074–2079.
- (6) (a) Shynkar, V. V.; Klymchenko, A. S.; Kunzelmann, C.; Dupontail, G.; Muller, C. D.; Demchenko, A. P.; Freyssinet, J.; Mely, Y. *J. Am. Chem. Soc.* **2007**, *129*, 2187–2193. (b) Li, X.; Qian, Y.; Wang, S.; Li, S.; Yang, G. *J. Phys. Chem. C* **2009**, *113*, 3862–3868. (c) Paul, B. K.; Guchhait, N. *J. Phys. Chem. B* **2010**, *114*, 12528–12540. (d) Zamotaiev, O. M.; Postupalenko, V. Y.; Shvadchak, V. V.; Pivovarenko, V. G.; Klymchenko, A. S.; Mély, Y. *Bioconjugate Chem.* **2011**, *22*, 101–107.
- (7) Park, S.; Kwon, J. E.; Kim, S. H.; Seo, J.; Chung, K.; Park, S.; Jang, D.; Medina, B. M.; Gierschner, J.; Park, S. Y. *J. Am. Chem. Soc.* **2009**, *131*, 14043–14049.
- (8) (a) Tang, K.; Chang, M.; Lin, T.; Pan, H.; Fang, T.; Chen, K.; Hung, W.; Hsu, Y.; Chou, P. *J. Am. Chem. Soc.* **2011**, *133*, 17738–17745. (b) Hsieh, C.-C.; Chou, P.-T.; Shih, C.-W.; Chuang, W.-T.; Chung, M.-W.; Lee, J.; Joo, T. *J. Am. Chem. Soc.* **2011**, *133*, 2932–2943.
- (9) Chuang, W.; Hsieh, C.; Lai, C.; Lai, C.; Shih, C.; Chen, K.; Hung, W.; Hsu, Y.; Chou, P. *J. Org. Chem.* **2011**, *76*, 8189–8202.
- (10) Stephan, J. S.; Grellmann, K. H. *J. Phys. Chem.* **1995**, *99*, 10066–10068.
- (11) Vázquez, S. R.; Rodríguez, M. C. R.; Mosquera, M.; Rodríguez-Prieto, F. *J. Phys. Chem. A* **2007**, *111*, 1814–1826.
- (12) Park, S.; Kwon, O.; Lee, Y.; Jang, D.; Park, S. Y. *J. Phys. Chem. A* **2007**, *111*, 9649–9653.

- (13) (a) Kim, C. H.; Joo, T. *Phys. Chem. Chem. Phys.* **2009**, *11*, 10266–10269. (b) Kim, C. H.; Park, J.; Seo, J.; Park, S. Y.; Joo, T. *J. Phys. Chem. A* **2010**, *114*, 5618–5629.
- (14) (a) Lukeman, M.; Wan, P. *Chem. Commun.* **2001**, 1004–1005. (b) Lukeman, M.; Wan, P. *J. Am. Chem. Soc.* **2002**, *124*, 9458–9464. (c) Lukeman, M.; Wan, P. *J. Am. Chem. Soc.* **2003**, *125*, 1164–1165. (d) Flegel, M.; Lukeman, M.; Huck, L.; Wan, P. *J. Am. Chem. Soc.* **2004**, *126*, 7890–7897. (e) Basaric, N.; Wan, P. *J. Org. Chem.* **2006**, *71*, 2677–2686. (f) Basaric, N.; Wan, P. *Photochem. Photobiol. Sci.* **2006**, *5*, 656–664. (g) Wang, Y.-H.; Wan, P. *Photochem. Photobiol. Sci.* **2011**, *10*, 1934–1944.
- (15) Zhao, G.; Han, K. *Acc. Chem. Res.* **2012**, *45*, 404–413.
- (16) Ikegami, M.; Arai, T. *J. Chem. Soc., Perkin Trans.* **2002**, *2*, 1296–1301.
- (17) Brewer, W. E.; Martinez, M. L.; Chou, P. *J. Phys. Chem.* **1990**, *94*, 1915–1918.
- (18) Iijima, T.; Momotake, A.; Shinohara, Y.; Sato, T.; Nishimura, Y.; Arai, T. *J. Phys. Chem. A* **2010**, *114*, 1603–1609.
- (19) Chung, M.; Lin, T.; Hsieh, C.; Tang, K.; Fu, H.; Chou, P.; Yang, S.; Chi, Y. *J. Phys. Chem. A* **2010**, *114*, 7886–7891.
- (20) Hanson, K.; Patel, Niral.; Whited, M. T.; Djurovich, P. I.; Thompson, M. E. *Org. Lett.* **2011**, *13*, 1598–1601.
- (21) Yogo, T.; Urano, Y.; Ishitsuka, Y.; Maniwa, F.; Nagano, T. *J. Am. Chem. Soc.* **2005**, *127*, 12162–12163.
- (22) Wu, Yi.; Zhen, Y.; Ma, Y.; Zheng, R.; Wang, Z.; Fu, H. *J. Phys. Chem. Lett.* **2010**, *1*, 2499–2502.
- (23) (a) Adarsh, N.; Avirah, R. R.; Ramaiah, D. *Org. Lett.* **2010**, *12*, 5720–5723. (b) Gorman, A.; Killoran, J.; O'Shea, C.; Kenna, T.; Gallagher, W. M.; O'Shea, D. F. *J. Am. Chem. Soc.* **2004**, *126*, 10619–10631.
- (24) (a) Wu, W.; Guo, H.; Wu, W.; Ji, S.; Zhao, J. *J. Org. Chem.* **2011**, *76*, 7056–7064. (b) Chen, Y.; Zhao, J.; Xie, L.; Guo, H.; Li, Q. *RSC Adv.* **2012**, *2*, 3942–3953. (c) Wu, W.; Zhao, J.; Guo, H.; Sun, J.; Ji, S.; Wang, Z. *Chem.—Eur. J.* **2012**, *18*, 1961–1968. (d) Huang, L.; Yu, X.; Wu, W.; Zhao, J. *Org. Lett.* **2012**, *14*, 2594–2597.
- (25) (a) Cakmak, Y.; Kolemen, S.; Duman, S.; Dede, Y.; Dolen, Y.; Kilic, B.; Kostereli, Z.; Yildirim, L. T.; Dogan, A. L.; Guc, D.; Akkaya, E. U. *Angew. Chem., Int. Ed.* **2011**, *50*, 11937–11941. (b) Duman, S.; Cakmak, Y.; Kolemen, S.; Akkaya, E. U.; Dede, Y. *J. Org. Chem.* **2012**, *77*, 4516–4527. (c) Cakmak, Y.; Akkaya, E. U. *Org. Lett.* **2009**, *11*, 85–88. (d) Buyukcikir, O.; Bozdemir, O. A.; Kolemen, S.; Erbas, S.; Akkaya, E. U. *Org. Lett.* **2009**, *11*, 4644–4647. (e) Guliyev, R.; Coskun, A.; Akkaya, E. U. *J. Am. Chem. Soc.* **2009**, *131*, 9007–9013. (f) Coskun, A.; Deniz, E.; Akkaya, E. U. *Org. Lett.* **2005**, *7*, 5187–5189. (g) Bozdemir, O. A.; Sozmen, F.; Buyukcikir, O.; Guliyev, R.; Cakmak, Y.; Akkaya, E. U. *Org. Lett.* **2010**, *12*, 1400–1403. (h) Coskun, A.; Akkaya, E. U. *J. Am. Chem. Soc.* **2006**, *128*, 14474–14475.
- (26) Takizawa, S.; Aboshi, R.; Murata, S. *Photochem. Photobiol. Sci.* **2011**, *10*, 895–903.
- (27) Uchoa, A. F.; Oliveira, K. T.; Baptista, M. S.; Bortoluzzi, A. J.; Iamamoto, Y.; Serraz, O. A. *J. Org. Chem.* **2011**, *76*, 8824–8832.
- (28) (a) Ulrich, G.; Ziessel, R.; Harriman, A. *Angew. Chem., Int. Ed.* **2008**, *47*, 1184–1201. (b) Ziessel, R.; Harriman, A. *Chem. Commun.* **2011**, *47*, 611–631.
- (29) Benniston, A. C.; Copley, G. *Phys. Chem. Chem. Phys.* **2009**, *11*, 4124–4131.
- (30) (a) Baruah, M.; Qin, W.; Vallée, R. A. L.; Beljonne, D.; Rohand, T.; Dehaen, W.; Boens, N. *Org. Lett.* **2005**, *7*, 4377–4380. (b) Baruah, M.; Qin, W.; Basarić, N.; De Borggraeve, W. M.; Boens, N. *J. Org. Chem.* **2005**, *70*, 4152–4157. (c) Baruah, M.; Qin, W.; Flors, C.; Hofkens, J.; Vallée, R. A. L.; Beljonne, D.; der Auweraer, M. V.; De Borggraeve, W. M.; Boens, N. *J. Phys. Chem. A* **2006**, *110*, 5998–6009. (d) Qin, W.; Rohand, T.; Dehaen, W.; Clifford, J. N.; Driesen, K.; Beljonne, D.; Averbeke, B. V.; der Auweraer, M. V.; Boens, N. *J. Phys. Chem. A* **2007**, *111*, 8588–8597. (e) Qin, W.; Baruah, M.; Sliwa, M.; der Auweraer, M. V.; De Borggraeve, W. M.; Beljonne, D.; Averbeke, B. V.; Boens, N. *J. Phys. Chem. A* **2008**, *112*, 6104–6114. (f) Leen, V.; Miscoria, D.; Yin, S.; Filarowski, A.; Ngongo, J. M.; der Auweraer, M. V.; Boens, N.; Dehaen, W. *J. Org. Chem.* **2011**, *76*, 8168–8176. (g) Cao, J.; Zhao, C.; Feng, P.; Zhang, Y.; Zhu, W. *RSC Adv.* **2012**, *2*, 418–420. (h) Cheng, T.; Xu, Y.; Zhang, S.; Zhu, W.; Qian, X.; Duan, L. *J. Am. Chem. Soc.* **2008**, *130*, 16160–16161.
- (31) (a) Bozdemir, O. A.; Erbas-Cakmak, S.; Ekiz, O. O.; Dana, A.; Akkaya, E. U. *Angew. Chem., Int. Ed.* **2011**, *50*, 10907–10912. (b) Sun, H.-B.; Liu, S.-J.; Ma, T.-C.; Song, N.-N.; Zhao, Q.; Huang, W. *New J. Chem.* **2011**, *35*, 1194–1197. (c) Lu, H.; Shimizu, S.; Mack, J.; Shen, Z.; Kobayashi, N. *Chem. Asian J.* **2011**, *6*, 1026–1037. (d) Descalzo, A. B.; Xu, H.-J.; Xue, Z.-L.; Hoffmann, K.; Shen, Z.; Weller, M. G.; You, X.-Z.; Rurack, K. *Org. Lett.* **2008**, *10*, 1581–1584.
- (32) (a) Wan, C.; Burghart, A.; Chen, J.; Bergström, F.; Johansson, L. B.; Wolford, M. F.; Kim, T. G.; Topp, M. R.; Hochstrasser, R. M.; Burgess, K. *Chem.—Eur. J.* **2003**, *9*, 4430–4441. (b) Loudet, A.; Burgess, K. *Chem. Rev.* **2007**, *107*, 4891–4932.
- (33) Singh-Rachford, T. N.; Castellano, F. N. *Coord. Chem. Rev.* **2010**, *254*, 2560–2573.
- (34) Zhao, J.; Ji, S.; Guo, H. *RSC Adv.* **2011**, *1*, 937–950.
- (35) Kwak, M. J.; Kim, Y. *Bull. Korean Chem. Soc.* **2009**, *30*, 2865–2866.
- (36) Baiz, C. R.; Ledford, S. J.; Kubarych, K. J.; Dunietz, B. D. *J. Phys. Chem. A* **2009**, *113*, 4862–4867.
- (37) Seo, J.; Kim, S.; Park, S. Y. *J. Am. Chem. Soc.* **2004**, *126*, 11154–11155.
- (38) Ceroni, P. *Chem.—Eur. J.* **2011**, *17*, 9560–9564.
- (39) Singh-Rachford, T. N.; Castellano, F. N. *J. Phys. Chem. A* **2009**, *113*, 5912–5917.
- (40) (a) Chen, H. C.; Hung, C. Y.; Wang, K. H.; Chen, H. L.; Fann, W. S.; Chien, F. C.; Chen, P.; Chow, T. J.; Hsu, C. P.; Sun, S. S. *Chem. Commun.* **2009**, 4064–4066. (b) Monguzzi, A.; Mezyk, J.; Scotognella, F.; Tubino, R.; Meinar, F. *Phys. Rev. B: Condens. Matter Mater. Phys.* **2008**, *78*, 195112. (c) Cheng, Y. Y.; Khoury, T.; Clady, R. G. C. R.; Tayebjee, M. J. Y.; Ekins-Daukes, N. J.; Crossley, M. J.; Schmidt, T. W. *Phys. Chem. Chem. Phys.* **2010**, *12*, 66–71. (d) Ji, S.; Wu, W.; Wu, W.; Guo, H.; Zhao, J. *Angew. Chem., Int. Ed.* **2011**, *50*, 1626–1629.
- (41) Ji, S.; Guo, H.; Wu, W.; Wu, W.; Zhao, J. *Angew. Chem., Int. Ed.* **2011**, *50*, 8283–8286.
- (42) Zhao, J.; Ji, S.; Wu, W.; Wu, W.; Guo, H.; Sun, J.; Sun, H.; Liu, Y.; Li, Q.; Huang, L. *RSC Adv.* **2012**, *2*, 1712–1728.
- (43) (a) Hanson, K.; Tamayo, A.; Diev, V. V.; Whited, M. T.; Djurovich, P. I.; Thompson, M. E. *Inorg. Chem.* **2010**, *49*, 6077–6084. (b) Sun, H.; Guo, H.; Wu, W.; Liu, X.; Zhao, J. *Dalton Trans.* **2011**, *40*, 7834–7841. (c) Liu, Y.; Wu, W.; Zhao, J.; Zhang, X.; Guo, H. *Dalton Trans.* **2011**, *40*, 9085–9089. (d) Wu, W.; Wu, W.; Ji, S.; Guo, H.; Zhao, J. *Dalton Trans.* **2011**, *40*, 5953–5963. (e) Sun, J.; Wu, W.; Guo, H.; Zhao, J. *Eur. J. Inorg. Chem.* **2011**, 3165–3173. (f) Huang, L.; Zeng, L.; Guo, H.; Wu, W.; Wu, W.; Ji, S.; Zhao, J. *Eur. J. Inorg. Chem.* **2011**, 4527–4533. (g) Wu, W.; Sun, J.; Ji, S.; Wu, W.; Zhao, J.; Guo, H. *Dalton Trans.* **2011**, *40*, 11550–11561. (h) Liu, Y.; Guo, H.; Zhao, J. *Chem. Commun.* **2011**, 11471–11473. (i) Wu, W.; Guo, H.; Wu, W.; Ji, S.; Zhao, J. *Inorg. Chem.* **2011**, *50*, 11446–11460.
- (44) Kowalczyk, T.; Lin, Z.; Voorhis, T. V. *J. Phys. Chem. A* **2010**, *114*, 10427–10434.
- (45) Zhao, G.; Liu, J.; Zhou, L.; Han, K. *J. Phys. Chem. B* **2007**, *111*, 8940–8945.
- (46) (a) Zhang, X.; Chi, L.; Ji, S.; Wu, Y.; Song, P.; Han, K.; Guo, H.; James, T. D.; Zhao, J. *J. Am. Chem. Soc.* **2009**, *131*, 17452–17463. (b) Han, F.; Chi, L.; Liang, X.; Ji, S.; Liu, S.; Zhou, F.; Wu, Y.; Han, K.; Zhao, J.; James, T. D. *J. Org. Chem.* **2009**, *74*, 1333–1336. (c) Zhang, X.; Wu, Y.; Ji, S.; Guo, H.; Song, P.; Han, K.; Wu, W.; Wu, W.; James, T. D.; Zhao, J. *J. Org. Chem.* **2010**, *75*, 2578–2588.
- (47) (a) Ji, S.; Yang, J.; Yang, Q.; Liu, S.; Chen, M.; Zhao, J. *J. Org. Chem.* **2009**, *74*, 4855–4865. (b) Guo, H.; Jing, Y.; Yuan, X.; Ji, S.; Zhao, J.; Li, X.; Kan, Y. *Org. Biomol. Chem.* **2011**, *9*, 3844–3853. (c) Shao, J.; Guo, H.; Ji, S.; Zhao, J. *Biosens. Bioelectron.* **2011**, *26*, 3012–3017. (d) Shao, J.; Sun, H.; Guo, H.; Ji, S.; Zhao, J.; Wu, W.; Yuan, X.; Zhang, C.; James, T. D. *Chem. Sci.* **2012**, *3*, 1049–1061.
- (48) Ji, S.; Guo, H.; Yuan, X.; Li, X.; Ding, H.; Gao, P.; Zhao, C.; Wu, W.; Wu, W.; Zhao, J. *Org. Lett.* **2010**, *12*, 2876–2879.

- (49) Zhou, F.; Shao, J.; Yang, Y.; Zhao, J.; Guo, H.; Li, X.; Ji, S.; Zhang, Z. *Eur. J. Org. Chem.* **2011**, 4773–4787.
- (50) Shao, J.; Ji, S.; Li, X.; Zhao, J.; Zhou, F.; Guo, H. *Eur. J. Org. Chem.* **2011**, 39, 6100–6109.
- (51) Deng, L.; Wu, W.; Guo, H.; Zhao, J.; Ji, S.; Zhang, X.; Yuan, X.; Zhang, C. *J. Org. Chem.* **2011**, 76, 9294–9304.
- (52) Kim, Y. H.; Rohb, S.; Junga, S.; Chunga, M.; Kimc, H. K.; Cho, D. W. *Photochem. Photobiol. Sci.* **2010**, 9, 722–729.
- (53) Turro, N. J.; Ramamurthy, V.; Scaiano, J. C. *Principles of Molecular Photochemistry: An Introduction*; University Science Books: Sausalito, CA, 2009.
- (54) (a) Yu, W.-S.; Cheng, C.-C.; Cheng, Y.-M.; Wu, P.-C.; Song, Y.-H.; Chi, Y.; Chou, P.-T. *J. Am. Chem. Soc.* **2003**, 125, 10800–10801. (b) Tsai, H.-H. G.; Sun, H.-L. S.; Tan, C.-J. *J. Phys. Chem. A* **2010**, 114, 4065–4079. (c) Ríos, M. A.; Ríos, M. C. *J. Phys. Chem. A* **1998**, 102, 1560–1567.
- (55) Papkovsky, D. B.; O’Riordan, T. C. *J. Fluoresc.* **2005**, 15, 569–584.
- (56) (a) Flamigni, L.; Barbier, A.; Sabatini, C.; Ventura, B.; Barigelletti, F. *Top. Curr. Chem.* **2007**, 281, 143–203. (b) Zhao, Q.; Li, F.; Huang, C. *Chem. Soc. Rev.* **2010**, 39, 3007–3030. (c) Chi, Y.; Chou, P.-T. *Chem. Soc. Rev.* **2010**, 39, 638–655.
- (57) Kořinek, M.; Dëdic, R.; Svoboda, A.; Hála, J. *J. Fluoresc.* **2004**, 14, 71–74.
- (58) (a) Zhang, D.; Wang, Y.; Xiao, Y.; Qian, S.; Qian, X. *Tetrahedron* **2009**, 65, 8099–8013. (b) Xu, Y.; Meng, J.; Meng, L.; Dong, Y.; Cheng, Y.; Zhu, C. *Chem.—Eur. J.* **2010**, 16, 12898–12903. (c) Tian, Y.; Chen, C.; Yang, C.; Young, A. C.; Jang, S.; Chen, W.; Jen, A. K. *Chem. Mater.* **2008**, 20, 1977–1987.
- (59) Frisch, M. J. et al. *Gaussian 09 Revision A.1*; Gaussian Inc.: Wallingford, CT, 2009.